JOURNAL OF AUTOMOTIVE POWERTRAIN AND TRANSPORTATION TECHNOLOGY
e-ISSN: 2821-286X

JAPTT

Vol. 4 No. 1 (2024) 18-29
https://publisher.uthm.edu.my/ojs/index.php/japtt

On the Scaling of Anthropometric Test Device (ATD) Finite Element Models

Ibrahim A. Rafukka[1]*, Barkawi B. Sahari[2], Abdulaziz. A. Nuraini[3], Arumugam Manohar[4]

[1] *Department of Mechanical Engineering, Faculty of Engineering, Bayero University, PMB 3011, Kano, NIGERIA*
[2] *Faculty of Engineering and Built Environment, UCSI University, Kuala Lumpur, MALAYSIA*
[3] *Department of Mechanical and Manufacturing Engineering, Faculty of Engineering, Universiti Putra Malaysia, 43400 UPM Serdang, Selangor, MALAYSIA*
[4] *Department of Orthopaedic Surgery, Faculty of Medicine and Health Sciences, Universiti Putra Malaysia, 43400 UPM Serdang, Selangor, MALAYSIA*

*Corresponding Author: ibrahimrafukka@yahoo.com
DOI: https:// doi.org/10.30880/japtt.2024.04.01.003

Article Info

Received: 18 March 2024
Accepted: 17 December 2024
Available online: 30 December 2024

Keywords

Anthropometry, crash dummy, finite element method, morphing, vehicle safety

Abstract

Crash dummies are the tools used to represent human beings in the assessment of vehicle safety performance. Current crash dummies are produced using US anthropometric data and children of various ages are not represented. This paper presents the application of morphing technique in generating crash dummy models to a given anthropometric data. The method was described using Hybrid III 3YO dummy model as an example. Morphing operation was applied to scale down the anthropometric dimensions of six year old Hybrid III (6YO HIII) dummy finite element (FE) model to that of three year old Hybrid III (3YO HIII). The morphed model was validated by comparing its biomechanical response data against experimental and simulation results from literature in a sled test based on the specification of Federal Motor Vehicle Safety Standard (FMVSS 213). The simulation results were found to be in good correlation with experimental and simulation results of sled test carried out using 3YO HIII dummy both qualitatively and quantitatively in x-head acceleration, x-chest acceleration and resultant upper neck moment and force. The curves of all the quantities show similarities in trends and the peak values were reasonably comparable to those in the literature results. The technique described in this study is therefore useful in developing child dummy for various age groups, percentiles as well as subject specific from existing FE model with short design time and reduced cost. The new dummy model developed could be used to evaluate three year old child injuries in motor vehicle crash simulations.

1. Introduction

Child vehicle safety is been given much concern by vehicle developers, researchers and society. Despite occupant safety systems available, child protection in vehicle crashes is still not optimum. It was recently shown that children 14 and younger account for 3% of total traffic fatalities in the United States [1]. Finite element modeling remains a useful tool in studying occupant injury risk and vehicle safety systems evaluation. Current crash dummies FE models represent only physical crash dummies available which are mainly limited to 50th percentiles of some specific age groups.

Mesh morphing provides easier way of reshaping shell and solid finite element model without going back to computer aided design (CAD) model for modification and re-meshing the model which is costly as it takes time. Idea of morphing and scaling of FE human models involves having a standard dummy as a base line from which other models are created. There is recently effort by Bio Mechanics Group from the Research and Development Department of a North America based Automotive OEM for applying morphing and scaling approach for generating standard and non-standard percentile human Body FE models. It was described as quick and systematic process of generating standard and non-standard FE dummies [2].

Research on crash dummy development is recently focused on vulnerable population such as children especially obese, pregnant women and elderly [3]– [5]. Computational modelling made it easier to create human models of specific anatomy. Due to unavailability of non-standard dummies e.g. 5th and 95th percentiles, it is important to drive other models using existing FE models such as Hybrid III dummy. Finite element model morphing and scaling is the best way of doing that. Morphing has been applied to develop age and sex specific thorax [6] and pedestrian models [7]. Kim et al [8] applied morphing method to scale human body model to an Obese Female. Hyncik et al [9] developed an algorithm to morph human body model. It was applied to morph adult model to a 13 year old child and the model was validated against experimental data. Scaling has been applied to children modelling from adult geometry for Multi body model for pedestrian safety [10], and scaling from adult human body models to three year old child [11], [12] and adult hybrid III dummy [13][13][14]. There is no study applied morphing on child ATD finite element models. Recent studies described developing new tools for scaling between different anthropometries as an active research area [7].

This study establishes the possibility of developing child ATD FE dummy models of various sizes using existing child dummy models. This will enable dummies representing children of various populations and age groups to be developed for the purpose of designing effective safety systems for them. It also provides simple way of developing dummies without making reference to existing physical crash dummies. Finite element model made it possible to amend material properties and parts geometry at lower cost compared to physical crash dummy modifications.

2. Methodology

2.1 Hybrid III 6YO and 3YO Models

Hybrid III 6 year old Finite Element Model Version: LST0.104.BETA shown in Fig. 1 is currently the latest child model in Livermore Software Technology Corporation (LSTC). The model has been validated against frontal crash tests with various restraint configurations [15]. It is used as the baseline model in this study. It was developed by LSTC in conjunction with National Crash Analysis Centre (NCAC). Its validation was based on the certification tests described in the Code of Federal Regulations, Title 49, Part 572, Sub-part N. It contains 199,102 nodes, 127,154 solid elements, 45,032 shell elements and 142 beam elements [18]. History beam elements and nodes are positioned in some specific locations of the body in order to provide the response data for the evaluation of occupant injury.

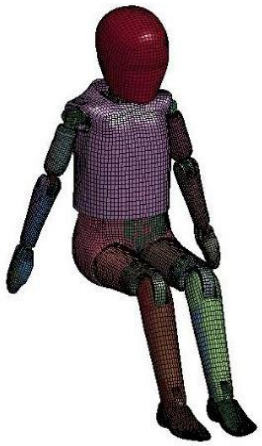

Fig. 1 *Hybrid III 6YO child dummy FE model [16]*

The 3YO Hybrid III dummy, which is the target model in this study was developed by humanetics in 1990s now Livermore Software Technology Corporation (LSTC) in corporation with National Highway Transport Safety Administration (NHTSA) and Society of Automotive Engineers (SAE) Biomechanics Committees. Hybrid III 3YO dummy was based on US child anthropometry collected back in eighties. It has a total number of 84,966 elements and was provided with accelerometers and load cells to measure injuries at various body locations [17].

2.2 Morphing Theory

Morphing involves scaling the nodes of body segment and repositioned it to reconnect back to the position it was before scaling. For the current case, the body external shape of both baseline and destination models (6YO HIII and 3YO HIII) was assumed to be the same, as such; a simple scaling morphing was applied. Guiding vectors are automatically selected in three dimensional morphing because morphed objects are more complex than in the two dimensional situation. Mesh scaling algorithm is embedded in FE software LS-PREPOST. Let's define vector:

$$x = [p\ q\ r\ ] \tag{1}$$

Where p, q and r are coordinates in three dimensional coordinate system of each node. Scaling the vector can be described using the transformation matrix, knowing the scaling factors:

$$R = \left[\lambda_x\ 0\ 0\ 0\ \lambda_y\ 0\ 0\ 0\ \lambda_z\ \right] \tag{2}$$

Where $\lambda_x, \lambda_y, and\ \lambda_z$ are scaling factors in x, y, and z direction defined as the ration of base line length to the destination length. Now:

$$x_{scaled} = Rx_{original} \tag{3}$$

Coordinate of each body segment was rotated to global coordinate system before morphing and then rotated back to their initial local coordinate system after operation. A translational adjustment is also done to reconnect back the morphed parts to their initial positions in order to maintain the original node joint distances.

Morphing is done in LS Prepost by constraining the parts to be morphed (Morph nodes) within a solid hex mesh (Constraining Element.). After Constrain has been activated, the hex mesh was transformed in any way, and the Morph nodes follow. The nodal coordinates are transformed based on their relative position within their containing solid element.

2.3 Dummy Scaling Procedure

Different scaling factors are assigned to different body segments in x, y and z-direction. Baseline model geometry (6YO HIII) was adapted freely to the target anthropometry (3YO HIII). Each dummy segment was constrained in morphing box. Scaling factors were calculated by dividing target anthropometry values L_{ti} by corresponding reference anthropometryL_{ri};

$$L_i = \frac{L_{ti}}{L_{ri}} \qquad i = x, y, z \tag{4}$$

x, was chosen to refer to the depth of body segment (e.g. head depth and chest depth for head and chest body segments respectively), y its lateral width (e.g. chest breadth for torso) and z its height (for example knee to sole length for lower leg).The dummy model body segments were constrained in morphing box as shown in Fig. 2.

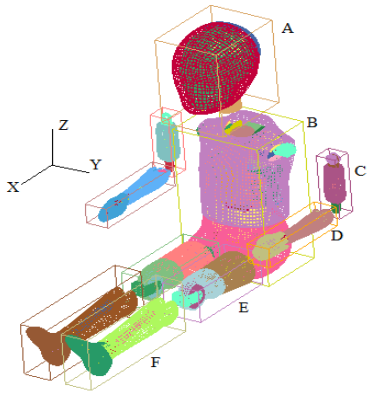

Fig. 2 *Dummy body segments in constraining element (morphing box)*

Scaling factors applied to various body segments are as listed in Table 1.

Table 1 *Size scale factors for 3-YO HIII dummy*

Body segments	3 YO HIII dummy		
	λ_x	λ_y	λ_z
Head-neck (A)	0.95	0.95	0.95
Torso (B)	0.93	0.93	0.75
Upper arm (C)	0.98	0.98	0.98
Lower arm(D)	0.89	0.89	0.89
Upper leg (E)	0.82	0.82	0.93
Lower leg (F)	0.83	0.83	0.83

The aim is to get a small or no difference for each anthropometric parameter. If the difference between the scaled model and target anthropometric dimension is large a correction scaling is carried out again. For easy measurement of body dimensions, nodes were selected as reference points to which all measurement before and after morphing were carried out. Table 2 shows anthropometric dimensions of 6YO HIII, 3YO HIII and Scaled 3YO HIII.

Table 2 *External anthropometric measurement used for morphing (all dimensions are in cm)*

Anthropometry	6YO Hybrid III (baseline model)	3YO Hybrid III (3YO HIII) [12] (Target)	Scaled 3YO Hybrid III FE model ($D_{H\,III}$)	% difference between D_{HII} and 3YO HIII
Head breadth	14.4	13.6	13.5	-0.7
Head depth	17.6	17.5	17.8	1.7
Head circumference	-	50.8	-	-
Chest breadth	19.7	-	15.6	-
Chest depth	15.7	14.6	14.9	2
Chest circumference	-	54.0	-	-
Shoulder height seated	41.9	31.5	33.5	-4.7
Shoulder breadth	-	24.4	23.9	-2
Shoulder to elbow	19.7	19.3	17.8	-7.7
Back of elbow to fingertip	28.7	25.5	23.8	-6.7
Waist circumference	-	54.0	-	-
Rump to knee length	38.5	29.2	29.3	0.34
Knee to sole length	32.6	27.2	28.0	3
Foot length	-	14.3	14.2	-0.7
Foot breadth	-	5.9	5.3	-10

Fig. 3 shows the 6YO HIII dummy FE model and the resulting three year old child dummy model obtained after scaling.

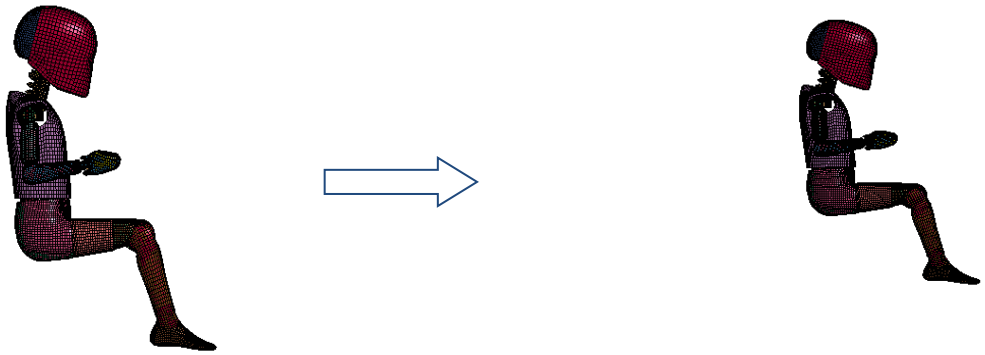

(a) **(b)**

Fig. 3 *6YO Hybrid III dummy (Base line model) (a) resulting 3YO Hybrid III dummy (Scaled model) (b)*

Mass and centre of gravity position of the target model was obtained by adjusting the mass density to meet with that of 3YO HIII dummy model. The dimensions and weight of the resulting target model were measured and compared to target anthropometry. The target mass of each body segment was achieved by scaling the density of each part contained in it using the same scaling factor. This is necessary in order to keep the centre of gravity CG in its initial position after mass reduction. The joint ranges of motion were assumed to be equal to those of the 6 year olds (6YO HIII). The weight of dummy body segments are presented in Table 3.

Table 3 *Body mass distribution of 3YO HIII and scaled 3YO HIII*

Body segment	3YO HIII (kg)	Scaled 3YO HIII ($D_{H\ III}$) (kg)
Head	2.72	2.61
Neck	0.79	0.31
Torso	7.00	7.47
Upper arm	0.44	0.45
Lower arm	0.46	0.38
Upper leg	1.01	0.89
Lower leg	0.61	0.55
Foot	0.31	0.21
Total	16.17	15.44

Morphing operation can affect the mesh quality of a morphed model because the displacements of the vertices were not taking care of during their movements. It can therefore cause some distortions of elements which affects their performance in finite element method analysis. The change in element quality due to morphing is not very significant as shown in Table 4. The morphed model met the mesh quality described in baseline model (6YO HIII). There was even a slight reduction in the percentage of element violating the criteria for skew and Jacobean conditions.

Table 4 *Element quality assessment of morphed model*

Condition	Criteria	Baseline model Element violating criteria (%)	Scaled model Element violating criteria (%)
Warpage angle	<10 deg	2.66	2.67
Aspect ratio	<10	0.44	0.44
skew	<45 deg	1.38	1.37
Jacobian	<0.6	5.57	5.28

2.4 Morphing Verification

The standard three year old child restraint seat (CRS) was modelled to accommodate the child dummy model in the sled test simulation. It is modelled as a rigid material with polypropylene material properties and a shell element of belytschko-Tsay type. The seat and belt CAD model were first drawn and meshed using Ls Prepost. It contains 3552 nodes, 3436 quadrilateral and 32 triangular elements. The mesh quality was tested and the aspect ratio and warpage angle was 4.92 and 8.74^0 respectively. Fabric material (MAT_FABRIC_34) with isotropic properties with belytschko-Tsay shell element was applied to five point harness belt. Both the seat and belt was modelled using 2 mm thickness membrane elements. The material parameters are presented in Table 5.

Table 5 *Material properties of child seat and belt [18]*

Parameter	Child seat	Five point harness
Density $\left(\frac{Kg}{m^3}\right)$	900	911.8
Elastic modulus (GPa)	1.2	6.27
Poisons ratio	0.3	0.3

Dummy was positioned into the CRS as shown in Fig. 4. Last raw of the five ends of the seat belt was constrained to rigid seat using constrained extra nodes sets so that it follows the acceleration prescribed in the negative x-direction.

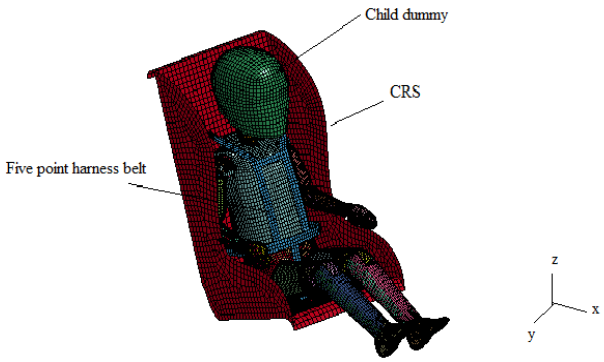

Fig. 4 *Child dummy model in CRS*

To ensure that the model represents the 3YO child, its response was compared with Hybrid III 3YO child dummy crash test results. In this case, the biomechanical response of the morphed model was compared with literature values. An acceleration pulse was applied to the rigid seat in the negative x-direction, while constrained in y and z direction for translation and rotation. The crash test was performed in LS DYNA software with an acceleration pulse shown in Fig. 5 at impact velocity of 13.34m/s, in accordance with FMVSS 213. The head and chest accelerations, resultant upper neck moments and forces were then measured and compared with experimental and simulation results from literature.

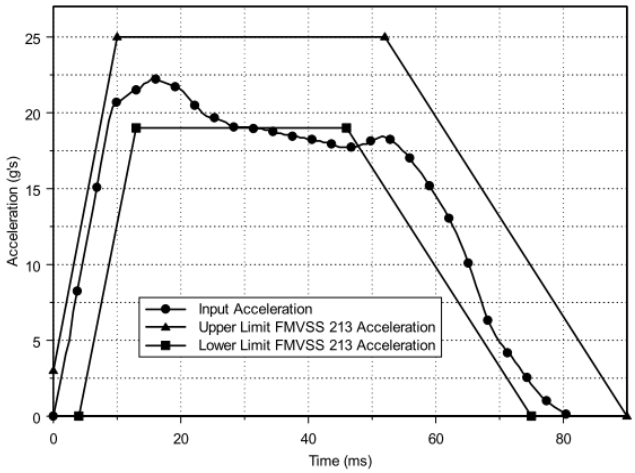

Fig. 5 *FMVSS 213 prescribed acceleration for sled test*

The dummy was positioned in the child seat and the constant downward gravity was applied in z-direction. Simulations were conducted in LS DYNA Solver and analysis was done for time duration of 150ms which is enough to observe the dummy response and interaction with child seat. AUTOMATIC_SURFACE_TO_SURFACE definition with static and dynamic friction coefficient of 0.3 and segment based soft contact option with a scale factor of 0.1 was defined between the dummy and both child seat and seat belt. The pre- and post-processing analysis was conducted with LS-Prepost (v4.2, LSTC, Livermore, CA, USA).

3. Scaled Dummy Model Validation

Due to difficulty in conducting crash tests using child PMHS or volunteer, child dummy response should at a minimum meet the requirements of HIII 3YO child dummy. In this study experimental and simulation results carried out using physical 3YO HIII dummy and HIII 3YO child dummy FE model from Turchi et al, 2004 [19], was used to validate the response of the morphed 3YO model (D_{HIII}) . Fig. 6 compares the kinematic response of D_{HIII} and physical dummy in a sled test conducted according to FMVSS 213. The figures depict an acceptable correlation between the simulation and experimental tests.

0 ms

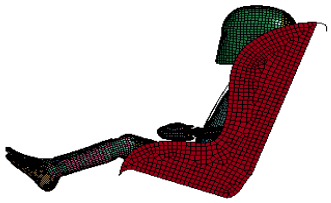

0ms

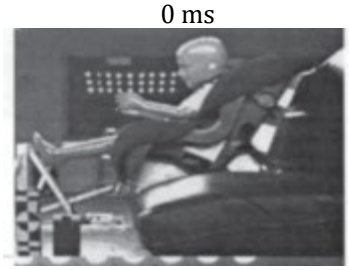

44 ms

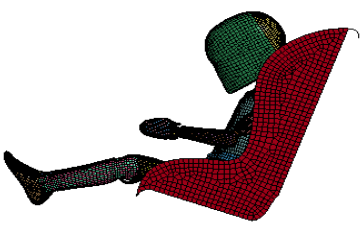

44 ms

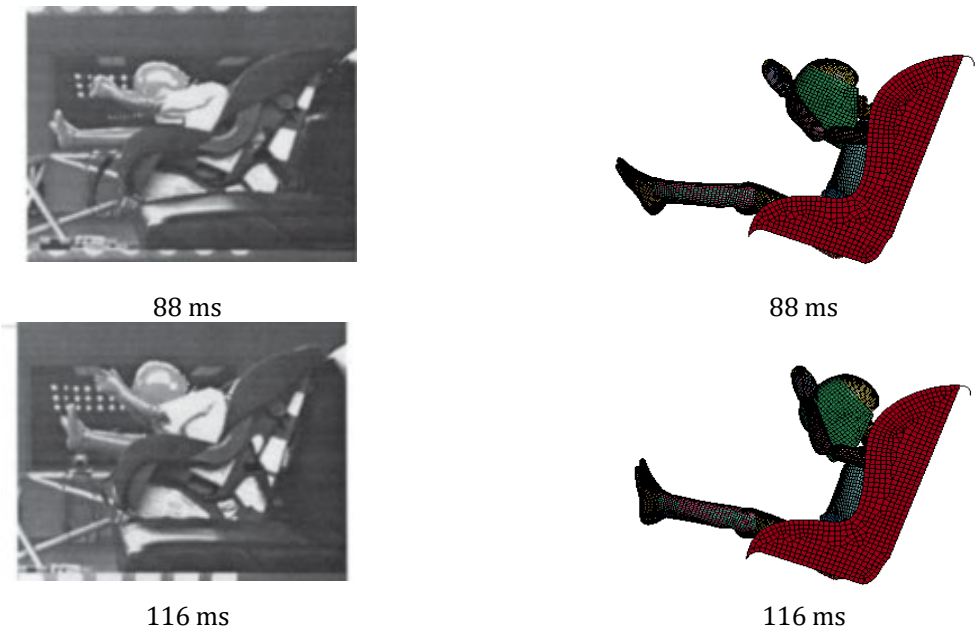

Fig. 6 *Qualitative comparison of scaled model* (D_{HIII}) *and HIII 3YO crash dummy from Turchi et al, 2004 [19]*

The numerical dummy seat was tilted to an angle of 20° in order to capture the physical dummy posture in sled test and this can be seen at time t= 0 ms as seen in Fig. 6. When the acceleration was applied to the child seat, upper and lower limbs of both dummies begin to extend forward, and neck flex as noticed at instant t=44ms. However, at t=88 ms, the physical dummy neck flex more than the numerical model does. This can be attributed to the rigid CRS model used and a five point harness belt with limited extension characteristics. Greatest lower limb extensions could be observed at t=116 ms for both numerical and physical dummies, with a little difference in the upper limbs and head position.

In general, the numerical model mimics the response of the physical dummy qualitatively. The differences in the response can be attributed to the approximations made in numerical modeling like the rigid seat, position of application of sled acceleration and joint stiffness that is assumed to be equals to that of 6YO HIII and the fact that the neck material properties were not adjusted.

3.1 Head X-Acceleration

The acceleration measured by accelerometer located at the head CoG in the impact direction is an important parameter in evaluating child injuries in a crash. Head x-acceleration-time history curve of D_{HIII} was compared with experimental and numerical test results which took place under the same conditions by Turchi et al. (2004) [19] as shown in Fig. 7. A channel frequency class (CFC) filter 1000 was applied to remove noise from the simulation results as was done in the physical test and in accordance with specifications [20]. There is good correlation in terms of the curve profile and peak timing between the experimental and simulation results while the peak value exhibit an acceptable difference of 26% as shown in Table 6. D_{HIII} shows excellent correlation with simulation results of Turchi et al, 2004 in terms of peak value with a difference of 2.9%. The minimum head x-acceleration of D_{HIII} and 3YO HIII simulation results was -33g and -34g respectively. The D_{HIII} and 3YO HIII simulation model show similar characteristics in the fact that each has two major peaks: small peak around 30ms and the main peak about 60ms. This is attributable to the similarities in the finite element characteristics.

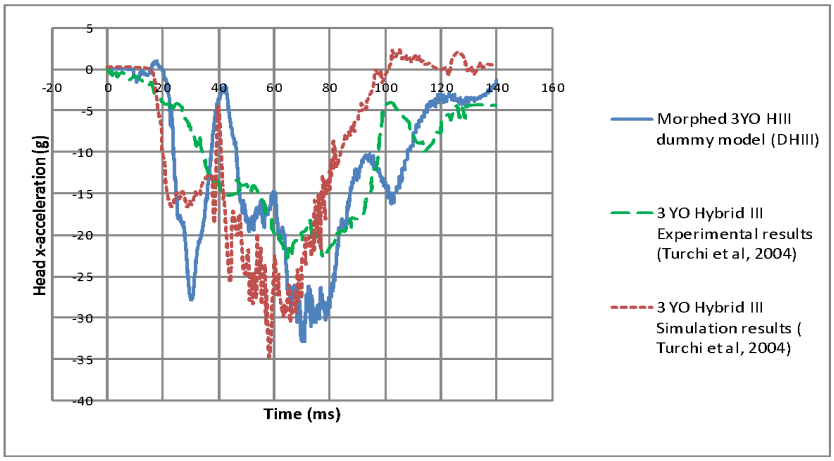

Fig. 7 *Comparison of head x-acceleration of* D_{HIII} *with experimental and simulation results of 3YO HIII from Turchi et al 2004 [19]*

In crash analysis and dummy modeling, the assessment is generally based on relative error of peak values of the injury parameters. Comparison of peak values has been applied in verification and validation of numerical models with experimental results by [21]– [25].

To date no criteria providing the percentage difference range for crash simulations and experimental results comparison. Judgment is often done subjectively. Some studies by [26]– [29] considered about 20% as really good, 20%-30% as fair and above 30% as poor. Recently, Wu et al. (2016) [30] considered a difference of 12.59% between peak value of numerical and experimental results as great agreement. Therefore, the present work considered 0%-20% as good and 20%-30% as acceptable or fair correlation in assessing the percentage difference between 3YO dummy simulation results and experimental and simulation results from literature.

3.2 Chest X-Acceleration

The x-component of chest acceleration is measured by accelerometer located on the spine of the dummy and the result was filtered using 180 CFC. Fig. 8 compares the D_{HIII} with experimental and simulation results from literature. All curves show similar profiles in the acceleration time history of chest in x-direction with fair correlation in peak acceleration timing which took place around 25 ms for the three tests. The minimum chest acceleration for D_{HIII} correlates well with experimental and simulation test of 3YO HIII dummy. The difference was 11.6% and 7.1% for experimental and simulation results as shown in Table 6.

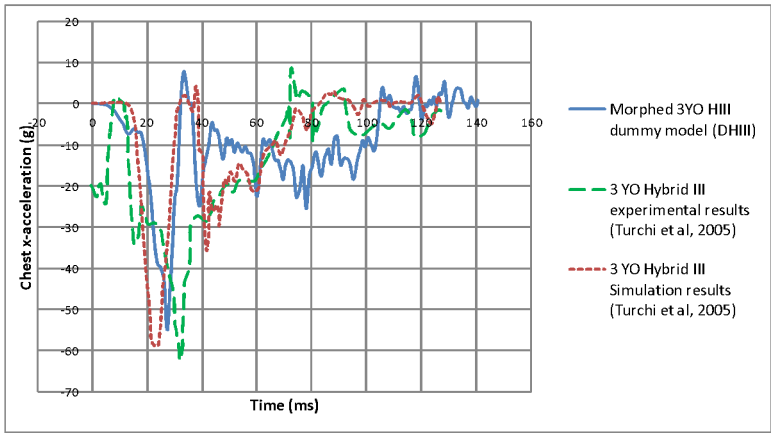

Fig. 8 *Comparison of chest x-acceleration of* D_{HIII} *with experimental and simulation results of 3YO HIII from Turchi et al. (2004) [19]*

3.3 Upper Neck Moment

The load cell located at the upper part of the dummy neck in the form of a beam element measures the neck bending moment. Resultant moment about y-axis is plotted against time as shown in Fig. 9.The data was filtered using 600 CFC as indicated in the 3YO HIII simulation test from Altenhof and Turchi (2004) [31]. The D_{HIII} experienced relatively high peak moment resultant of 43 Nm than the 3YO HIII dummy model with 36 Nm, but

both models show two notable peaks which notify similarities in the curve trends. An acceptable correlation in peak value was obtained from the two results with a difference of 19.4% as shown in Table 6. The higher peaks in the D_{HIII} may probably be due to possible differences in the simulation setups.

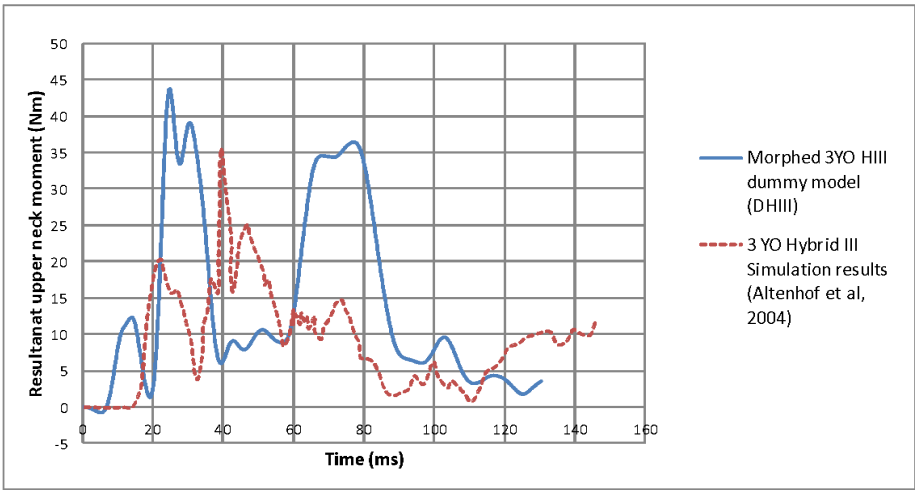

Fig. 9 *Comparison of resultant upper neck moment of* $\boldsymbol{D_{HIII}}$ *simulation results of 3YO HIII from Altenhof and Turchi (2004) [31]*

3.4 Upper Neck Force

The resultant neck force-time history measured by the upper neck load cell and filtered using 1000 CFC is shown in Fig. 10. Both models exhibited excellent correlation because the peaks for the 3YO HIII model and D_{HIII} are 1200 N and 1172 N respectively with a difference of 2.3% as shown in Table 6. Even though D_{HIII} peak appeared earlier, the two curves showed similar profile.

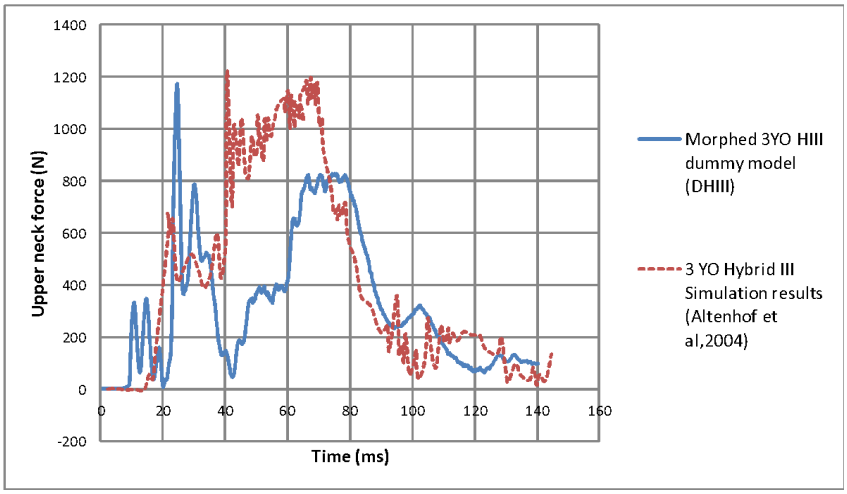

Fig. 10 *Comparison of resultant upper neck force of* $\boldsymbol{D_{HIII}}$ *with simulation results from from Altenhof and Turchi (2004) [31]*

The results of the D_{HIII} show good agreement with both experimental and simulation results using 3YO HIII dummy. This indicates the capability of the new dummy model (D_{HIII}) to measure injury parameters during crash as 3YO HIII can do. Considering all the simplifications of the model, the D_{HIII} can represent both physical and FE 3YO HIII model. It is very hardly to match the results of FE model with physical test in a simulation that was carried out using different parts like CRS, harness belt and other connections. In fact, matching results of two different FE models of the same dummy is highly difficult.

Table 6 *Comparison of D_{HIII} biomechanical response with experimental and simulation results of 3YO HIII*

Head acceleration (g)			Chest acceleration (g)			Upper neck moment (Nm)			Upper neck force (N)		
Exper. 3YO HIII	Simul. D_{HIII}	% diff.	Exper. 3YO HIII	Simul. D_{HIII}	% diff.	Simul. 3YO HIII	Simul. D_{HIII}	% diff.	Simul. 3YO HIII	Simul. D_{HIII}	% diff.
26	33	26	62	54.8	11.6	36	43	19.4	1200	1172	2.3
Simul. 3YO HIII	Simul. D_{HIII}		Simul. 3YO HIII	Simul. D_{HIII}							
34	33	2.9	59	54.8	7.1						

4. Conclusions

This study described the technique of scaling child dummy FE models to other anthropometries using morphing operation. Scaling 6YO HIII to 3YO HIII anthropometry was used as an example to demonstrate the technique. The morphed model developed by scaling 6YO HIII dummy model to 3YO HIII child dummy dimensions has been validated by the simulation and experimental results of 3YO HIII in a sled test. The dummy response matches relatively well for all the parameters compared. Overall results indicates that the proposed technique was valid and could therefore be applied to modeling dummies of various anthropometries without making reference to physical ones. This enables the vulnerable children like obsess and children of non-standard sizes to be modeled for the assessment of child restraint system and vehicle structures safety performance. Nigerian children that are not represented by current crash dummies could be modeled using morphing technique.

Acknowledgement

The authors would like to acknowledge Bayero University, Kano, Nigeria, Infrastructure University Kuala Lumpur (IUKL), Malaysia and Universiti Putra Malaysia (UPM), for their supports in works related to this paper.

Author Contribution

The authors confirm contribution to the paper as follows: ***Morphing, model verification and writing original draft:*** *Ibrahim A. Rafukka;* ***Supervision, correcting paper writing****: Barkawi B. Sahari; Abdulaziz Nuraini; Arumugam Manohar; All authors reviewed the results and approved the final version of the manuscript.*

References

[1] NHTSA. (2014). National Highway Traffic Safety Administration, Traffic Safety Facts, Children, 2012 Data DOT HS 812 011.

[2] DEP. (2015). Bio medical - detroit engineered products. Retrieved July 1, 2016, from http://www.depusa.com.

[3] Kim, J. E., Hsieh, M. H., Shum, P. C., Tubbs, R. S. & Allison, D. B. (2015). Risk and injury severity of obese child passengers in motor vehicle crashes, Obesity, 23, (3), 644–652.

[4] NHTSA. (2023). Traffic Safety Data, 2021 Data.

[5] Gu, X. and Zhou, Y. (2023). Analysis of Studies on Traffic Crashes Involving the Elderly: A survey of methods, influencing factors, and perspectives Analysis of Studies on Traffic Crashes Involving the Elderly. Int. Rev. Spat. Plan. Sustain. Dev., vol. 11 (January), 4–23.

[6] Schoell, S. L., Weaver, A. A., Vavalle, N. A., & Stitzel, J. D. (2014). Development of Age and Sex - Specific Thorax Finite Element Models. Ohio State University Injury Biomechanics Symposium, 1–13.

[7] Poulard, D., Chen, H., Crandall, J. R., Dziewo, T., Michal, P. & Panzer, M. B. (2015). Component-level Biofidelity Assessment of Morphed Pedestrian Finite Element Models. IRC-15-65 IRCOBI Conference, 577–593.

[8] Kim, J., Lee, I., Kim, T. & Kim, H. (2015). Validation of Abdominal Characteristics under Lap-belt Loadings using Human Body Model Morphed to an Obese Female. IRC-15-23 IRCOBI Conference, 133–135.

[9] Hyncik, L., Novacek, V., Blaha, P., Chvojka, O. & Krejci, P. (2007). On scaling of human body models. Appl. Comput. Mech., Volume 1, 63–76.

[10] Liu, X. J. and Yang, J. K. (2002). Development of Child Pedestrian Mathematical Models and Evaluation with Accident Reconstruction. Traffic Inj. Prev., 3 (4), 321–329.

[11] Koizumi, T., Tsujiuchi, N., Taki, N., Forbes, P. A. & De Lange, R. (2007). Development and Impact Analysis of 3-Year-Old Child FE Human Model. Conference Proceedings of the Society for Experimental Mechanics Series, 25th Conference and Exposition on Structural Dynamics 2007, IMAC-XXV, Orlando, FL, USA, 1–3.

[12] Mizuno, K., Iwata, K., Deguchi, T., Ikami, T. and Kubota, M. (2005). Development of a three-year-old child FE model. Traffic Inj. Prev., 6 (May 2014), 361–371.

[13] Ly, A. H., Nguyen, B. D. & Nguyen, H. A. (2021). Methodology for scaling finite element dummy and validation of a Hybrid III dummy model in crashworthiness simulation. Sci. Technol. Dev. J. – Eng. Technol., 2(December 2019).

[14] Abdul Samad M. S. and Mohd Nor, M. K. (2022). A comparative analysis between a newly Malaysian size ATD and the current Hybrid III ATD in frontal impact. Cogent Eng., 9(1).

[15] Wu, K. D., Boyle, J., Orton, K., Manary, N. R., Reed, M. A. & Kliunich, M. P. (2023). A Modeling Study on Child Occupant Safety With Unconventional Seating Configurations. (Report No. DOT HS 813 434), National Highway Traffic Safety Administration.

[16] LSTC. (2011). Download LSTC Dummy and Barrier Models for LS-DYNA. Retrieved July 2, 2016, from http://www.lstc.com/download/dummy_and_barrier_models

[17] FTSS. (2008). FTSS Hybrid III 3 Year Old Dummy Model – LS-DYNA.

[18] Kapoor, T., Altenhof, W., Wang, Q. & Howard, A. (2006). Injury potential of a three-year-old Hybrid III dummy in forward and rearward facing positions under CMVSS 208 testing conditions. Accid. Anal. Prev., vol. 38, 786–800.

[19] Turchi, R., Altenhof, W., Kapoor, T. & Howard, A. (2004). An investigation into the head and neck injury potential of three-year-old children in forward and rearward facing child safety seats. Int. J. Crashworthiness, 9, (4), 419–431.

[20] NHTSA. (2011). National Highway Traffic Safety Administration-part 572.146-subpart P-3-year-old child crash test dummy, alpha version.

[21] Prange, M. T., Luck, J. F., Dibb, A., Van Ee, C., Nightingale, R. W. & Myers, B. S. (2004). Mechanical properties and anthropometry of the human infant head. Stapp Car Crash J., vol. 48, 279–299.

[22] Loyd, A. M., Nightingale, R. W., Song, Y., Luck, J. F., Cutcliffe, H., Myers, B. S. & Bass, C. D.(2012). Impact Properties of Adult and ATD Heads. in IRCOBI Conference Proceedings, 2012, no. 507, 552–564.

[23] Ash, J., Abdelilah, Y., Crandall, J., Parent, D., Sherwood, C. & Kallieris, D. (2009). Comparison of anthropomorphic test dummies with a pediatric cadaver restrained by a three-point belt in frontal sled tests. 21st International Technical Conference on the Enhanced Safety of Vehicles, 1–14.

[24] Lai, X., Lin, Z. & Culiere, P. (2011). Development of a finite element PAM-CRASH model of Hybrid III anthropomorphic test device with high fidelity. The 22nd International Conference on the Enhanced Safety Vehicles, 1–10.

[25] Li, Z., Luo, X. & Zhang, J. (2013). Development/global validation of a 6-month-old pediatric head finite element model and application in investigation of drop-induced infant head injury. Comput. Methods Programs Biomed., 112 (3), 309–319.

[26] Wang, Q. and Gabler, H. C. (2008). Review of correlation methods for evaluating finite element simulations of impact injury risk. Biomed. Sci. Instrum., vol. 44, 268–273.

[27] Geers, T. L. (1984). An objective error measure for the comparison of calculated and measured transient response histories. Shock Vib. Bull., 54 (2), 99–107.

[28] Mongiardini, M., Ray, M. H., Anghileri, M. & Milano, P. (2009). Development of a Software for the Comparison of Curves During the Verification and Validation of Numerical Models. 7th European LS-DYNA Conference.

[29] Schwer, L. E. (2007). Validation metrics for response histories: Perspectives and case studies. Eng. Comput., 23(4), 295–309.

[30] Wu, S., Zheng, G., Sun, G., Liu, Q., Li, G. & Li, Q. (2016). On design of multi-cell thin-wall structures for crashworthiness. Int. J. Impact Eng., vol. 88, 102–117.

[31] Altenhof W. and Turchi, R. (2004). A Numerical Investigation into HIC and Nij of Children for Forward and Rearward Facing Configurations in a Child Restraint System. 8th International LS-DYNA Users Conference, no. 2, 69–86.